coatings

MDPI

Article

Influence of Conditions for Production and Thermo-Chemical Treatment of Al_2O_3 Coatings on Wettability and Energy State of Their Surface

Mateusz Niedźwiedź, Władysław Skoneczny * and Marek Bara

Institute of Materials Engineering, Faculty of Science and Technology, University of Silesia in Katowice, 40-007 Katowice, Poland; mateusz.niedzwiedz@us.edu.pl (M.N.); marek.bara@us.edu.pl (M.B.)

* Correspondence: wladyslaw.skoneczny@us.edu.pl; Tel.: +48-32-368563

Received: 26 June 2020; Accepted: 13 July 2020; Published: 15 July 2020

Abstract: This article presents the influence of the anodizing parameters and thermo-chemical treatment of Al_2O_3 coatings made on aluminum alloy EN AW-5251 on the surface free energy. The oxide coating was produced by DC (Direct Current) anodizing in a ternary electrolyte. The thermo-chemical treatment of the oxide coatings was carried out using distilled water, sodium dichromate and sodium sulphate. Micrographs of the surface of the Al_2O_3 coatings were characterized using a scanning microscope (SEM). The chemical composition of the oxide coatings was identified using EDS (Energy Dispersive X-ray Spectroscopy) microanalysis. Surface free energy (SFE) calculations were performed by the Owens–Wendt method, based on wetting angle measurements made using the sessile drop technique. The highest value of surface free energy for the only anodized coatings was 46.57 mJ/m^2, and the lowest was 37.66 mJ/m^2. The contact angle measurement with glycerine was 98.06° ± 2.62°, suggesting a hydrophobic surface. The thermo-chemical treatment of the oxide coatings for most samples contributed to a significant increase in SFE, while reducing the contact angle with water. The highest value of surface free energy for the coatings after thermo-chemical treatment was 77.94 mJ/m^2, while the lowest was 34.98 mJ/m^2. Taking into account the contact angle measurement with glycerine, it was possible to obtain hydrophobic layers with the highest angle of 109.82° ± 4.79° for the sample after thermal treatment in sodium sulphate.

Keywords: aluminum oxide layers; surface morphology; thermo-chemical treatment

1. Introduction

Nowadays, when a common criterion for material selection is its weight to strength ratio, and when great importance is attached to environmentally friendly solutions, aluminum has become very widely used in material engineering [1]. The most important advantages of aluminum are undoubtedly its low weight in relation to strength, high electrical and thermal conductivity, ease of forming in all machining processes such as rolling and extrusion, considerable corrosion resistance and almost 100% recyclability without losing its properties [2–4]. In its pure form, aluminum, in addition to the number of advantages, also has significant disadvantages, which are its low melting point and low absolute strength [5]. In order to minimize these disadvantages, aluminum is combined with elements such as copper, silicon or magnesium to form durable alloys [6]. The industries that most often use aluminum and its alloys are the automotive, aviation and shipbuilding industries [7–10].

In order to better protect aluminum alloys against mechanical damage and corrosion, the process of so-called anodizing (oxidation) is used [11,12]. Anodizing aluminum and its alloys is an electrochemical process consisting of creating an oxide coating on the surface of an alloy, usually with a thickness of a few to several dozen micrometers [13]. The anodized coating is many times harder than pure

aluminum or aluminum alloys (1700 to 2000 HV Al_2O_3 hardness at about 30 HV for pure aluminum and 200 HV for PA9 alloy) [14,15]. During the electrochemical process, the formation of the oxide coating occurs at the expense of substrate loss. This results in very good adhesion of the coating to the aluminum substrate. The most commonly used type of anodizing is hard DC (Direct Current) anodizing. During the process, as the coating thickness increases, the anodizing voltage increases [16]. The beginning of the DC anodizing process is characterized by a rapid increase in voltage, necessary to break through the compact and thin (0.01–0.1 μm thick) natural barrier layer, also called the barrier layer [17]. In the next stage of the process, the voltage decreases. When the minimum value is reached, the barrier layer is rebuilt at the oxide–electrolyte interface. The voltage increases again over time due to the formation of pores and their further deepening as the thickness of the Al_2O_3 coating increases, up to a maximum thickness of approximately 150 μm [18,19]. The oxide coating produced during anodizing ideally reaches the form of regular pores arranged in the shape of a hexagonal system, along with a thin barrier film in direct contact with the aluminum substrate. The oxide pore sizes mainly depend on the anodizing method used, but also on the process parameters. A high temperature and long anodizing time increase the solubility of the oxide, while creating a porous coating with poorer protective properties [20,21].

For better corrosion protection and sealing of the absorbent oxide coating while maintaining its advantages, thermo-chemical treatment is used [22]. As a result of processing in the Al_2O_3 coating, aluminum oxide is transformed into hydrated forms such as γ-Al $(OH)_3$ hydrargillite and γ-AlOOH boehmite. The transformation occurs due to swelling of the walls of the Al_2O_3 cells owing to their hydration, as a result of which the pores are closed, and a smooth surface is created [23]. During thermo-chemical treatment, the process of producing a pseudo-boehmite sublayer on the surface may also occur; this happens most often when the process is short (several minutes), but also at high temperatures [24].

Researchers have investigated the thermo-chemical treatment of oxide coatings, but the research lacks reference to the impact of this process on the wettability of the Al_2O_3 layers [25,26]. The porosity of oxide coatings has a significant impact on their energy state, and thus the properties enabling the repulsion (hydrophobicity) and attraction (hydrophilicity) of water molecules [27]. That is why studies on the wettability of oxide coatings produced as a result of anodizing and thermo-chemical treatment are so important. Nowadays, the energy state is a very important feature of materials. Materials with hydrophobic properties, i.e., those exhibiting low wettability, repelling water particles, are widely used in surface engineering as self-cleaning or anti-icing materials [28,29]. Materials with high wettability are also in high demand, or, in other words, attracting water particles (hydrophilic); they are used in photovoltaic panels, biomaterials and wherever it is important to reduce friction [30–32]. A surface is considered hydrophobic when the water contact angle is greater than 90°. The conventional name for surfaces reaching contact angles over 150° is ultrahydrophobicity. The opposite of hydrophobicity is hydrophilicity and occurs when the contact angle on the surface is less than 90° [33].

Many authors have carried out research on the modification of Al_2O_3 layers by thermo-chemical treatment. In [34], 6061 aluminum alloy was anodized at a constant voltage in an electrolyte at the temperature of 273 K. A 15% H_2SO_4 solution was used as the electrolyte, the anodizing time was 60 min, and a voltage of 15–30 V was used. Then, each of the produced layers were modified by immersion in stearic acid at the temperature of 353 K for 45 min, successively in ethanol at the temperature of 343 K. The whole process was completed by drying in an oven at the temperature of 253 K. The authors of the work managed to obtain hydrophobic surfaces; the contact angles were 138°–152° depending on the anodizing voltage used. In subsequent studies, researchers conducted studies using two-stage anodizing on 1050 aluminium alloy at the temperature of 273 K. As the electrolyte, 10.5% and 1% solutions of H_3PO_4 were used; the process was carried out using the constant voltage method at voltages in the range of 160–195 V for 60 min in Stage 1 and 15–300 min in Stage 2. After Stage 1 of anodizing, the layers were immersed in a solution of 6% H_3PO_4, 1.8% CrO_3 and deionized water at the temperature of 333 K. Wet chemical etching was carried out in a 5% solution of H_3PO_4 at the

temperature of 333 K for 60–150 min. In the next step, the layers were sonicated in acetone for 10 min, then dried in an oven at the temperature of 343 K for 360 min and modified by immersion in a 5% $C_{12}H_{24}O_2$ solution for 90 min. The last stage of layer modification was spraying with silane and dried at the temperature of 413 K for 30 min. Thanks to the use of lauric acid, the contact angles were higher by 5°–30°, while thanks to silane spraying, a hydrophobic coating with a contact angle of 146° was obtained [35]. In the next cited article, researchers also dealt with constant voltage anodizing using a $C_2H_2O_4$ electrolyte. The anodizing time was 420 min at the voltage of 40 V. The layers were modified by immersion in an 0.3% polytetrafluoroethylene solution and then cured at room temperature. In the next stage, the samples were immersed in a solution of 1.8% H_2CrO_4 and 6% H_3PO_4 at the temperature of 338 K for 300 min. Contact angles of 120° before immersion and 160° after immersion in a polytetrafluoroethylene solution were obtained [36]. Another article that can be cited is research based on two-stage constant voltage anodizing. Anodizing was carried out at the temperature of 275 K in a 1% H_3PO_4 solution. A voltage of 194 V was applied for 60 min in the 1st stage and 300 min in the 2nd stage. After completing Stage 1, the layers were immersed in a 6% H_3PO_4 solution and a 2% H_2CrO_4 solution at the temperature of 323 K for 40 min. After anodizing was completed, the layers were immersion modified in deionized H_2O at the temperature of 373 K for 1 min. This process mainly involved preparing the substrate for subsequent treatments. The samples were then dried at the temperature of 323 K and finally treated with hexamethyldisilane vapor (HMDS) for 240 and 540 min. As a result of the performed modifications, contact angles of 139°–153° were obtained (depending on the number and duration of HMDS cycles) [37].

In all the cited publications, the researchers focused mainly on the modification of oxide coatings produced as a result of constant voltage anodizing. In the next publication, the coatings were prepared using the DC method for 120 min at a current density of 1–2 A/dm^2. The process was carried out in a 5% H_3PO_4 solution at a temperature of 283–293 K. Some of the samples were plasma treated and all of them were immersed in trichloro octadecylsilane-hexane for 120 min as well as being washed with hexane and oven dried at the temperature of 333 K. Wetting angles of 152° (without plasma treatment) and 157° (after plasma treatment) were obtained [38].

After analyzing the literature, it was found that most of the world research on the wettability of Al_2O_3 coatings is mainly based on the modification of the coating by applying additional layers to their surfaces. There is a lack of research in this area regarding the impact of the anodizing parameters before and after applying thermo-chemical treatment and the impact of the compounds used for this treatment on the contact angles, and thus the energy state of the surface of the coatings, which makes our research innovative. The studies presented below focused mainly on the impact of the anodizing parameters (current density, electrolyte temperature, anodizing time) and the impact of the thermo-chemical treatment carried out with various compounds (water, sodium dichromate, sodium sulphate) on the contact angles of oxide coatings. Measurement of the contact angles allowed the energy state of the layers to be determined by calculating the surface free energy.

2. Materials and Methods

2.1. Research Material

The research material was Al_2O_3 coatings made on aluminum alloy EN AW-5251 by means of hard DC anodizing. The aluminum alloy used has a high magnesium content, which contributes to such properties as good ductility, high corrosion resistance and high weldability. This alloy is most often used in the construction of aircraft and marine structures.

The samples for producing the oxide coatings had a surface area of 0.1 dm^2. Before proceeding with the anodizing process, each sample was etched in a 5% KOH solution for 20 min, followed by a whitening process in a 10% HNO_3 solution for 5 min. The temperature of the used solutions was 296 K. At the end of each process, the samples were rinsed in distilled water. The coatings were produced in the DC anodizing process using a GPR-25H30D power supply. The process was carried out in

variable production conditions (current density, anodizing time), at a variable electrolyte temperature (anodizing without thermo-chemical treatment) and a constant electrolyte temperature for the samples subjected to thermo-chemical treatment after the anodizing process. A ternary electrolyte consisting of an 18% sulphuric acid solution (33 mL/L), oxalic acid (30 g/L), and phthalic acid (76 g/L) was used for the anodizing process. During anodizing, the electrolyte was mixed mechanically at 100 rpm, the direction of rotation was changed every 10 min.

The studies were carried out according to a statistically determined poly-selective experiment plan. Hartley's plan was applied for three input factors based on a hypercube, for which coefficient $\alpha = 1$. Table 1 presents the list of factors on a natural and standard scale for coatings produced in the anodizing process without thermo-chemical treatment.

Table 1. List of factors on natural and standard scale for coatings produced in anodizing process without thermo-chemical treatment.

Sample	Controlled Factors					
	On a Natural Scale			On a Standard Scale		
	Current Density j [A/dm^2]	Electrolyte Temperature T [K]	Process Time t [min]	×1	×2	×3
01A	2	293	90	−1	−1	1
01B	4	293	30	1	−1	−1
01C	2	303	30	−1	1	−1
01D	4	303	90	1	1	1
01E	2	298	60	−1	0	0
01F	4	298	60	1	0	0
01G	3	293	60	0	−1	0
01H	3	303	60	0	1	0
01I	3	298	30	0	0	−1
01J	3	298	90	0	0	1
01K	3	298	60	0	0	0

Table 2 presents the list of factors on a natural and standard scale for coatings produced in the process of anodizing and thermo-chemical treatment. The thermo-chemical treatment was carried out after thorough rinsing of the samples in distilled water. The anodizing process was carried out at the constant electrolyte temperature of 298 K. Thermo-chemical treatment was carried out in solutions of distilled water, sodium dichromate and sodium sulphate. For each compound, the treatments lasted 60 min, the temperature of the solutions was 371 K.

Table 2. List of factors on natural and standard scale for coatings produced in anodizing process and thermo-chemical treatment.

Sample	Controlled Factors					
	On a Natural Scale			On a Standard Scale		
	Current Density j [A/dm^2]	Compound for Thermo-Chemical Treatment (Density) [g/cm^3]	Process Time t [min]	×1	×2	×3
02A	2	Water (0.998)	90	−1	−1	1
02B	4	Water (0.998)	30	1	−1	−1
02C	2	Sodium dichromate (2.52)	30	−1	1	−1
02D	4	Sodium dichromate (2.52)	90	1	1	1
02E	2	Sodium sulphate (1.46)	60	−1	0	0
02F	4	Sodium sulphate (1.46)	60	1	0	0
02G	3	Water (0.998)	60	0	−1	0
02H	3	Sodium dichromate (2.52)	60	0	1	0
02I	3	Sodium sulphate (1.46)	30	0	0	−1
02J	3	Sodium sulphate (1.46)	90	0	0	1
02K	3	Sodium sulphate (1.46)	60	0	0	0

2.2. Research Methodology

The thickness of the oxide coatings was measured by the contact method using a Dualscope MP40 instrument (Helmut Fischer GmbH + Co.KG, Sindelfingen, Germany), which uses the eddy current method for measurement. Ten measurements were taken along the entire length of the samples with three repetitions and the mean values were calculated along with deviations.

Using a Hitachi S-4700 scanning microscope (Hitachi, Tokyo, Japan), a micrograph of the morphology of the Al_2O_3 coatings was made. A magnification of 50,000× was used to observe the surface. Before further studies were carried out, the surfaces were sprayed with carbon to remove electrons struck during interaction of the microscope beam. Analysis of the chemical composition of the oxide coatings was carried out using a Noran Vantage EDS (Energy Dispersive X-ray Spectroscopy) system attached to the Hitachi S-4700 scanning microscope.

Contact angle measurements were performed using four liquids, two polar (water and glycerine) and two non-polar (α-bromonaphthalene and diiodomethane). Ten drops of each liquid were applied to each of the investigated coatings using an 0.5 µL micropipette over the entire length of the sample. Photographs of each drop were taken with a camera, which were then exported to a computer. The software used allowed the marking of three extreme points on the drop photograph, which enabled automatic measurement of the contact angle. The smallest and largest angles were rejected, and the other eight angle values were used to calculate the average contact angle of a particular coating. Surface free energy was calculated by the Owens–Wendt method using one polar (water) and one non-polar liquid (α-bromonaphthalene). Calculations using the Owens–Wendt method were carried out based on the equation:

$$\gamma_s = \gamma_s{}^d + \gamma_s{}^p \quad (1)$$

where γ_s is the surface free energy of the solid, $\gamma_s{}^d$ is the surface free energy (SFE) dispersion component of the examined materials, and $\gamma_s{}^p$ is the SFE polar component of the investigated materials.

3. Results and Discussion

Table 3 presents the average results of thickness measurements of the oxide coatings produced in the anodizing process (without thermo-chemical treatment).

Table 3. List of Al_2O_3 coating thicknesses produced in anodizing process (without thermo-chemical treatment).

Sample	Oxide Layers Thickness *d* [µm]	Deviation [µm]
01A	51.3	0.94
01B	33.1	0.90
01C	16.9	0.22
01D	94.8	0.66
01E	32.6	0.45
01F	67.6	0.42
01G	53.1	1.12
01H	51.2	0.91
01I	25.2	0.33
01J	75.9	0.47
01K	51.4	0.96

The measurements showed significant changes in the thickness of the oxide coatings resulting from the use of different anodizing parameters. The thickness of the coatings depends on the process time, current density and electrolyte temperature. An increase in anodizing time at a constant current density and electrolyte temperature causes a significant increase in the coating thickness (samples 01I, 01J, 01K). As the current density increased, while the electrolyte time and temperature remained constant, a significant increase in coating thickness was also observed (samples 01E, 01F, 01K). In both cases,

the increase in coating thickness is due to the increasing value of the electric charge. An increase in electrolyte temperature, while maintaining a constant anodizing time and current density, contributes to a decrease in coating thickness, which is caused by an increase in Al_2O_3 secondary solubility along with an increase in electrolyte temperature (samples 01G, 01H, 01K).

Table 4 presents the average results of thickness measurements of oxide coatings produced in the anodizing process and thermo-chemical treatment.

Table 4. Summary of Al_2O_3 coating thickness produced in anodizing process and thermo-chemical treatment.

Sample	Oxide Layers Thickness *d* [μm]	Deviation [μm]
02A	51.1	0.58
02B	33.5	0.81
02C	16.4	0.31
02D	98.6	5.79
02E	34.0	0.53
02F	68.7	0.59
02G	48.9	0.57
02H	51.9	0.45
02I	27.5	0.47
02J	77.1	1.31
02K	52.1	0.19

Comparing the measurements of the thickness of the oxide coatings before and after the thermo-chemical treatment produced under the same anodizing conditions, it can be stated that the treatment causes a slight increase in the thickness of the oxide coating (comparison of samples 01I, 01J, 01K with samples 02 I, 02J, 0.2 K). Confirmation of this can also be seen by comparing samples 01E, 01F, 01K with samples 02E, 02F, 02K. The increase in the layer thickness after thermo-chemical treatment is insignificant and varies within 1.5 μm. As in the case of unmodified coatings, after the thermo-chemical treatment, the dependence of the increase in Al_2O_3 thickness on the increase in current density and the time of the anodizing process can also be seen. Table 5 shows the contact angle values measured using distilled water and α-bromonaphthalene. Table 6 shows the contact angle values measured using glycerine and diiodomethane. The measurements were made on coatings produced during anodizing without thermo-chemical treatment. Depending on the anodizing parameters, different contact angle values were obtained. The highest contact angle for polar liquids (distilled water, glycerine) was obtained for the 01D sample produced at the current density of 4 A/dm^2 for 90 min at the electrolyte temperature of 303 K. The lowest value was obtained for the 01J sample produced at the current density of 3 A/dm^2 for 90 min at the electrolyte temperature of 298 K. Considering the values of the contact angles of the coatings measured using glycerine, sample 01D is a hydrophobic surface with a contact angle of 98.06° ± 2.62°.

Table 7 contains the contact angle values measured using distilled water and α-bromonaphthalene. Table 8 shows the contact angle values measured using glycerine and diiodomethane. The Al_2O_3 coatings underwent thermo-chemical treatment after previous anodizing. The highest value of contact angle measured with distilled water was obtained for sample 02E produced at the current density of 2 A/dm^2 for 60 min, then subjected to thermo-chemical treatment in sodium sulphate. The smallest contact angle value was obtained for the 02D sample produced at the current density of 4 A/dm^2 for 90 min, subjected to thermo-chemical treatment in sodium dichromate. The produced coating was highly hydrophilic—the measured angle was only 8.62° ± 2.02°. Considering the second polar liquid (glycerine), the smallest contact angle value was also measured for the 02D sample; however, the largest value was as much as 109.82° ± 4.79°—the highly hydrophobic surface was measured on the 02K sample produced at the current density of 3 A/dm^2 for 60 min and then subjected to thermo-chemical treatment in sodium sulphate. Sample 02E also showed hydrophobic properties—its contact angle was 92.78 ± 6.62°. Thermo-chemical treatment of the Al_2O_3 coatings contributed to a significant change in

the wettability of the measured surfaces. In the case of the sample anodized at the current density of 3 A/dm^2 for 60 min, the thermo-chemical treatment in sodium sulphate contributed to an increase in the contact angle from 73.86° to 81.14° for water and from 71.95° to 109.82° for glycerine, creating a highly hydrophobic surface. Furthermore, the thermo-chemical treatment of samples 01E, 01F, 01K in sodium sulphate contributed to a significant reduction in wettability (a higher contact angle) for glycerine. A reduction in the electrolyte temperature during anodizing from 303 to 298 K and the thermo-chemical treatment process in sodium dichromate of samples 01C, 01D, 01H contributed to a very large increase in the wettability of the coatings, creating surfaces with strong hydrophilic properties, both using water and glycerine. An increase in the electrolyte temperature during anodizing from 293 to 298 K for samples 01A, 01B, 01G and the thermo-chemical treatment process using water resulted in a significant reduction in the contact angle.

Table 9 presents the surface free energy values calculated by the Owens–Wendt method. Wetting angles measured using distilled water and α-bromonaphthalene using the sessile drop technique were used for the calculations. The angles were measured on Al_2O_3 coating without thermo-chemical treatment.

Table 5. Wetting angles of oxide coatings produced in the anodizing process (without thermo-chemical treatment) for distilled water and α-bromonaphthalene.

Sample	Contact Angle (Distilled Water) [°]	Deviation [°]	Contact Angle (α-Bromonaphthalene) [°]	Deviation [°]
01A	74.60	2.22	22.70	3.28
01B	81.61	7.07	33.54	4.26
01C	72.55	6.35	28.82	3.22
01D	85.84	3.36	33.76	7.86
01E	76.80	2.26	27.26	1.34
01F	80.76	5.78	36.25	2.23
01G	84.06	5.71	27.51	3.46
01H	79.23	4.80	27.09	1.83
01I	80.52	5.94	26.69	1.34
01J	69.68	3.57	31.88	4.93
01K	73.86	2.83	24.97	4.12

Table 6. Wetting angles of oxide coatings produced in the anodizing process (without thermo-chemical treatment) for glycerine and diiodomethane.

Sample	Contact Angle (Glycerin) [°]	Deviation [°]	Contact Angle (Diiodomethane) [°]	Deviation [°]
01A	72.10	3.54	44.95	6.56
01B	80.67	2.09	50.44	3.09
01C	83.09	6.06	47.39	1.53
01D	98.06	2.62	64.09	5.07
01E	77.38	1.23	47.87	3.52
01F	85.98	5.29	47.96	4.34
01G	79.55	3.17	49.66	6.29
01H	76.68	4.08	49.16	3.56
01I	79.75	3.45	48.48	1.95
01J	71.19	2.81	52.65	2.51
01K	71.95	4.70	51.68	3.23

Table 7. Wetting angles of oxide coatings produced in anodizing process and thermo-chemical treatment for distilled water and α-bromonaphthalene.

Sample	Contact Angle (Distilled Water) [°]	Deviation [°]	Contact Angle (α-Bromonaphthalene) [°]	Deviation [°]
02A	56.81	2.48	13.93	2.64
02B	60.44	1.97	17.67	2.62
02C	27.44	4.13	15.89	1.63
02D	8.62	2.02	9.54	2.74
02E	89.61	6.34	44.83	5.26
02F	63.18	3.55	22.15	3.21
02G	71.29	11.02	18.89	3.56
02H	22.55	1.95	14.44	2.81
02I	61.74	4.15	38.33	3.88
02J	52.77	6.94	22.63	2.77
02K	81.14	6.16	37.86	3.63

Table 8. Wetting angles of oxide coatings produced in the anodizing process and thermo-chemical treatment for glycerine and diiodomethane.

Sample	Contact Angle (Glycerin) [°]	Deviation [°]	Contact Angle (Diiodomethane) [°]	Deviation [°]
02A	73.84	5.01	30.88	5.52
02B	84.47	4.97	34.57	1.90
02C	54.11	7.56	32.05	3.35
02D	27.67	2.53	17.88	2.47
02E	92.78	6.62	59.71	10.68
02F	88.74	7.26	36.89	3.22
02G	85.40	6.81	37.24	5.47
02H	41.19	5.01	23.33	3.86
02I	88.25	3.05	52.99	6.19
02J	64.60	4.74	41.79	3.43
02K	109.82	4.79	57.25	5.38

Table 9. Surface free energy values of Al_2O_3 coatings without thermo-chemical treatment.

Sample	SFE Owens-Wendt [mJ/m^2]
01A	43.15
01B	41.35
01C	46.12
01D	40.06
01E	44.85
01F	40.73
01G	37.66
01H	39.56
01I	43.75
01J	46.57
01K	40.84

The highest value of surface free energy was determined for the 01J sample, i.e., for the coating characterized by the smallest contact angle for water, while the lowest SFE value was determined for the surface characterized by one of the highest contact angles for water (84.06°)—sample 01G. After the calculations, it can be stated that on oxide coatings without thermo-chemical treatment, the contact angles show inverse proportionality to the value of surface free energy. Three-dimensional graphs were made to visualize the effect of the anodizing parameters on SFE (Figure 1).

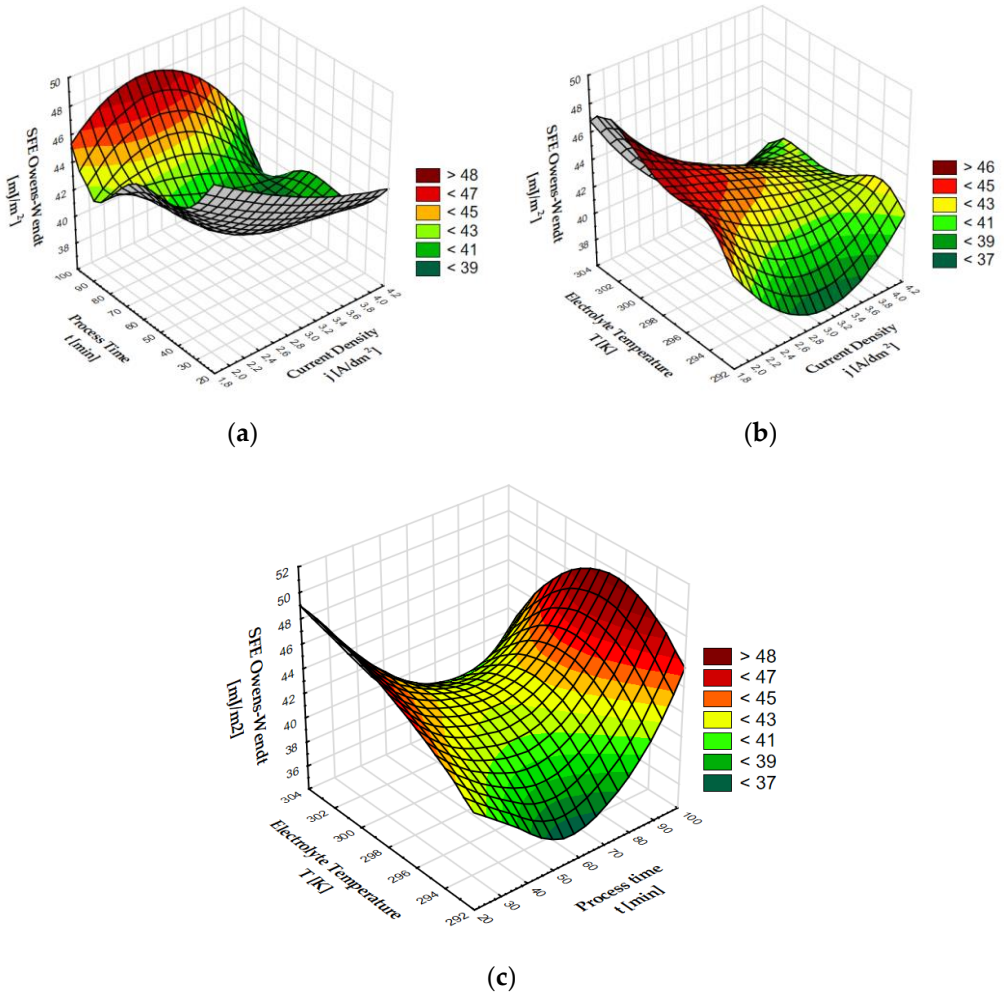

Figure 1. Surface free energy (SFE) dependence on: (**a**) process time and current density, (**b**) electrolyte temperature and current density, (**c**) electrolyte temperature and process time.

By analyzing the impact of the process time and current density on SFE, it can be seen that the highest values of surface free energy of over 44 [mJ/m^2] were exhibited by a coating produced within 100 min and at the current density of 3 A/dm^2. Values over 40 [mJ/m^2] were also observed for coatings produced within 30 min for all the current density values. The graph showing the effect of electrolyte temperature and current density on SFE shows a clear increase in the surface free energy value in the middle of the electrolyte temperature axis for a current density of about 2 A/dm^2. The lowest values < 39 [mJ/m^2] were attained for the current density of 3 A/dm^2 and electrolyte temperature around 293 K. The next graph presents the dependence of SFE on the electrolyte temperature and process time. The highest values > 44 [mJ/m^2] were found at the beginning and end of the process time axis at values in the middle of the electrolyte temperature axis (298 K).

Table 10 shows the SFE calculated for coatings after thermo-chemical treatment. The calculations were carried out using the Owen–Wendt method based on the contact angles of distilled water and α-bromonaphthalene.

Table 10. Values of surface free energy of Al_2O_3 coatings after thermo-chemical treatment.

Sample	SFE Owens-Wendt [mJ/m^2]
02A	56.60
02B	54.19
02C	71.73
02D	77.94
02E	34.98
02F	52.01
02G	48.91
02H	73.85
02I	48.92
02J	57.49
02K	40.06

Sample 02D showed the highest surface free energy; this is a coating which, after anodizing, was subjected to thermo-chemical treatment in sodium dichromate. The coating also has the lowest contact angle for water (8.62°) and for glycerine (27.67°). The lowest SFE value was calculated for sample 02E, which has the highest contact angle for water (89.61°) and one of the highest for glycerine (92.78°). As with the Al_2O_3 coatings without modification, the contact angles of the coatings after thermo-chemical treatment show an inverse proportionality to the value of surface free energy. Figure 2 presents 3D graphs of the dependence of the anodizing parameters and compounds used for thermo-chemical treatment on the SFE value.

The surface free energy of coatings after thermo-chemical treatment varies depending on the process time and current density. The highest SFE values > 75 mJ/m^2 were found at the intersection of the end of the process time axis (about 90 min) and the end of the current density axis (about 4 A/dm^2). A clear increase can also be seen at the intersection of a current density of about 2 A/dm^2 and a process time of about 30 min. By analyzing the impact of the current density and the compound used for thermochemical treatment, it can be stated that the greatest impact on the increase in the SFE value is the use of sodium dichromate in the coating modification process. When using sodium dichromate, a clear increase in surface free energy is visible in the entire current density range, with a peak value > 76 mJ/m^2 for a current density of about 4 A/dm^2. A clear decrease in the SFE value can be seen for sodium sulphate at the current density of 2 A/dm^2. The graph showing the dependence of SFE on the time of the process and the compound used for thermochemical treatment shows a clear maximum SFE value > 76 mJ/m^2 for sodium dichromate, decreasing with the time of the process. Surface free energy values > 56 mJ/m^2 are also visible in the case of anodized coatings that underwent thermo-chemical treatment in water for about 90 min. A clear decrease in the SFE value < 44 mJ/m^2 is visible in the middle of the graph for anodized coatings modified in the sodium sulphate solution for about 60 min.

Figure 3 presents surface morphology micrographs taken with a scanning microscope of selected oxide coatings with the largest differences in the contact angle and SFE. A 50,000× magnification was used for all the morphology micrographs.

The micrographs show surface porosity, which is characteristic of Al_2O_3 coatings. There are significant differences in the size of the nanopores, which depend on both the anodizing time and the current density used in the anodizing process.

Figure 4 presents micrographs of the surface morphology of layers anodized and thermo-chemically treated in sodium dichromate and sodium sulphate.

The thermo-chemical treatment of the 02D sample carried out in sodium dichromate contributed to complete sealing of the porous Al_2O_3 coating and the formation of a high sodium content sublayer. On the surfaces of the 02E and 02K samples, which after the anodizing process were subjected to thermo-chemical treatment in sodium sulphate, complete coverage of the oxide coating surface with a kind of crosslinked structure is noticeable.

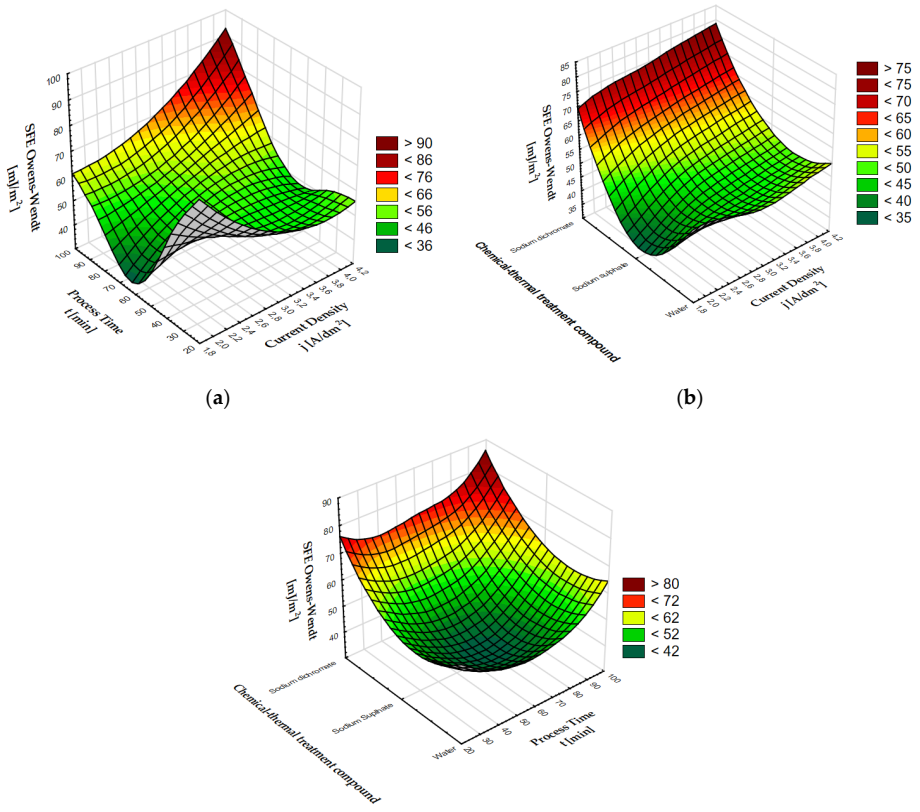

Figure 2. SFE dependence on: (**a**) process time and current density, (**b**) chemical compounds used in coating modification and current density, (**c**) chemical compounds used in coating modification and process time.

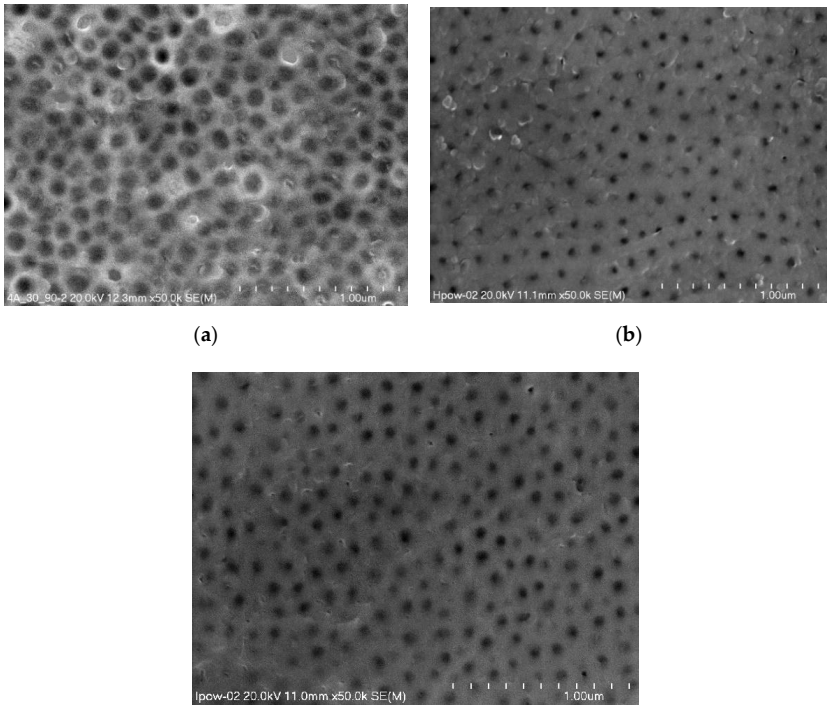

Figure 3. Surface morphology micrographs of oxide coatings without thermo-chemical treatment: (**a**) Sample 01D, (**b**) Sample 01H, (**c**) Sample 01J.

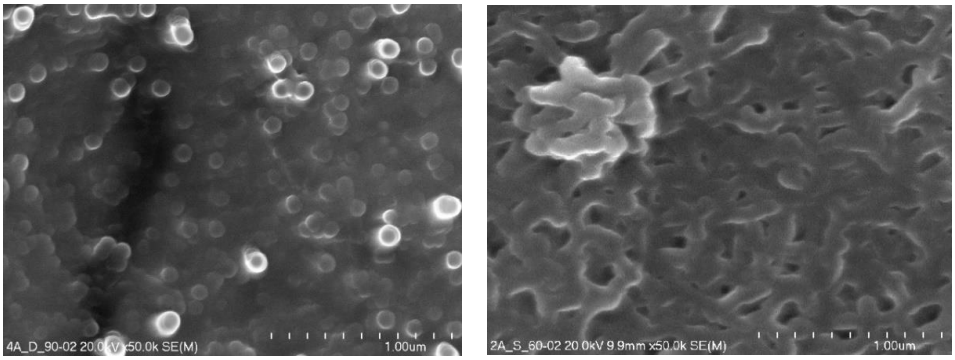

(**a**) (**b**)

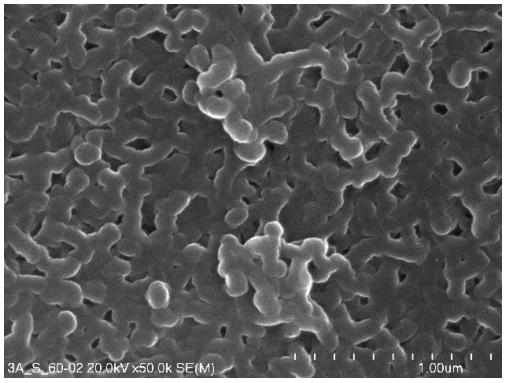

(**c**)

Figure 4. Surface morphology micrographs of oxide layers after thermo-chemical treatment: (**a**) Sample 02D, (**b**) Sample 02E, (**c**) Sample 02K.

Table 11 summarizes the chemical composition of the oxide coatings produced in the DC anodizing process without the thermo-chemical process.

Table 11. Chemical composition analysis of Al_2O_3 coatings without thermo-chemical process.

Sample	Atomic Aluminum Content [%]	Error of Aluminum Content [%]	Atomic Oxygen Content [%]	Error of Oxygen Content [%]
01D	54.52	±0.30	43.94	±0.68
01H	56.23	±0.21	44.25	±0.54
01J	55.90	±0.23	43.49	±0.51

Samples with significant differences in the values of surface free energy and contact angle were selected for analysis. The atomic content of both aluminum and oxygen in the selected coatings are very similar. An increase in aluminum content was observed for the samples with a smaller Al_2O_3 coating thickness. The increased aluminum content is due to the shorter distance between the coating surface and the substrate. The values presented in the table are very similar to stoichiometric calculations of the alumina chemical composition.

Figure 5 presents SEM micrographs for samples 02D, 02E, 02K together with the marked field used for chemical composition analysis. Figure 6 shows the EDS spectrum for the 02D, 02E, 02K samples with chemical composition analysis.

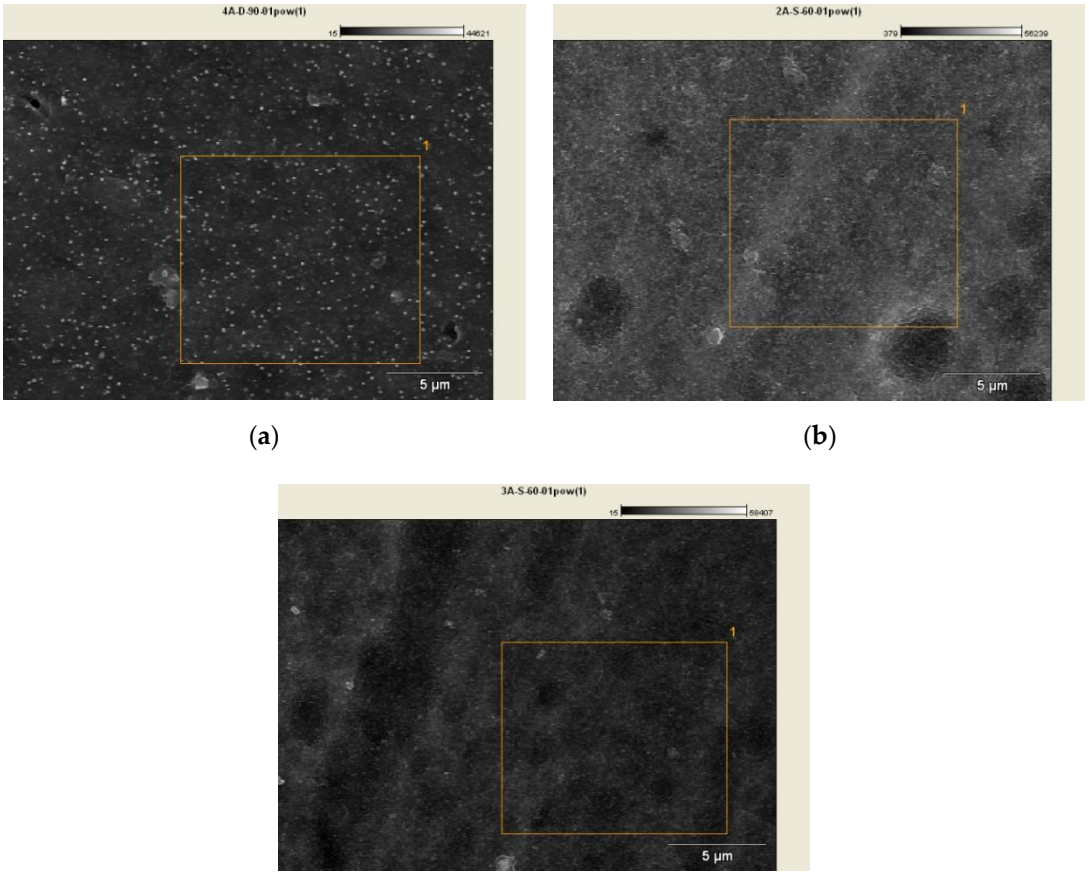

(**a**) (**b**)

(**c**)

Figure 5. SEM micrographs with chemical analysis field marked: (**a**) Sample 02D, (**b**) Sample 02E, (**c**) Sample 02K.

The coating composition of sample 02D is characterized by a high content of oxygen, at the same time reducing the content of aluminum. Thermo-chemical treatment in sodium dichromate contributed to the building of over 18% sodium compounds on the surface. On the surfaces of the 02E and 02K samples modified in sodium sulphate, a reduction in oxygen content for about 2% sulphur was shown.

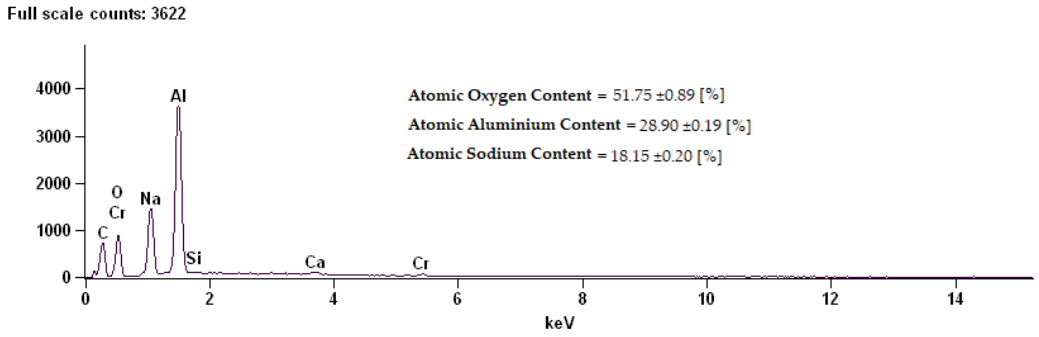

(**a**)

Figure 6. *Cont.*

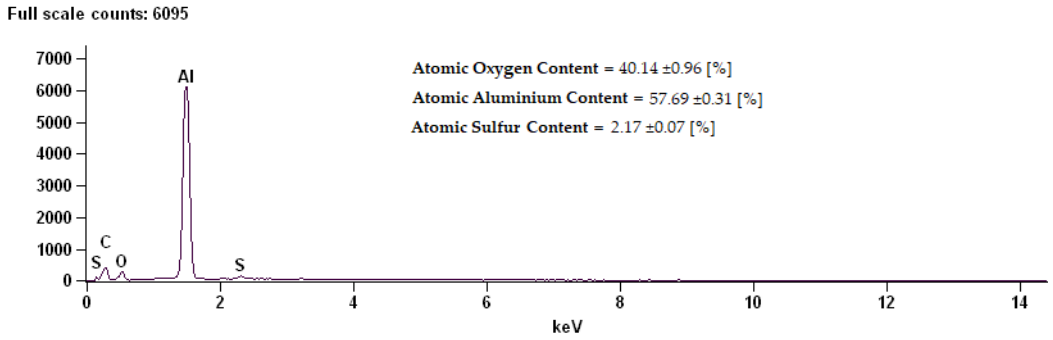

(**b**)

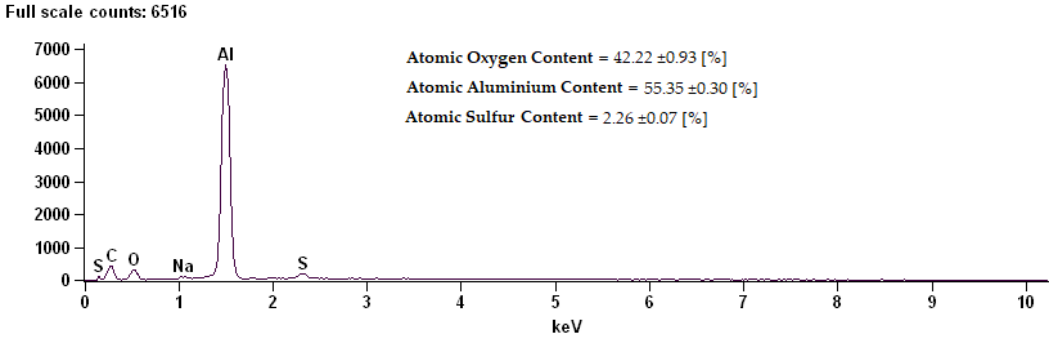

(**c**)

Figure 6. EDS (Energy Dispersive X-ray Spectroscopy) spectrum along with chemical analysis for samples: (**a**) Sample 02D, (**b**) Sample 02E, (**c**) Sample 02K.

4. Conclusions

Based on the conducted studies, it can be concluded that both the anodizing parameters and thermo-chemical treatment have a significant impact on the wettability of Al_2O_3 coating surfaces, and thus their energy state. By controlling the anodizing parameters (current density, electrolyte temperature, process time), a hydrophobic surface with a contact angle of 98.06° ± 2.62° was obtained for the 01D sample using glycerine as the measuring liquid. The 01D sample oxide coating also achieved the highest contact angle with distilled water. The coating was produced at the current density of 4 A/dm^2 for 90 min at the electrolyte temperature of 303 K. The lowest contact angle value was obtained by the coating produced at the current density of 3 A/dm^2 for 90 min at the electrolyte temperature of 298 K—sample 01J.

The second part of the research focused on the modification of the Al_2O_3 coatings by chemical compounds through thermo-chemical treatment. A very clear effect of thermo-chemical treatment on the values of contact angles was noticed. The highest contact angle value measured using distilled water was obtained by sample 02E modified in sodium sulphate. The smallest contact angle value was obtained by a sample modified in sodium dichromate. The coating modified in sodium dichromate showed strongly hydrophilic values; the measured angle was only 8.62° ± 2.02°. For the 02K sample modified in sodium sulphate, the contact angle measurements with glycerine revealed an angle of 109.82° ± 4.79° (a strongly hydrophobic surface). Moreover, sample 02E exhibited hydrophobic properties; the contact angle for this coating was 92.78° ± 6.62°. The thermo-chemical treatment in sodium sulphate of the 02K sample increased the contact angle from 73.86° to 81.14° for water and from 71.95° to 109.82° for glycerine, creating a highly hydrophobic surface. The modification also contributed to a significant reduction in wettability for glycerine. The reduction in electrolyte temperature in the anodizing process of the coatings modified in sodium dichromate contributed to a very large increase in the wettability of the coatings, creating surfaces with strong hydrophilic

properties, both when measuring with distilled water and glycerine. The increase in electrolyte temperature during anodizing from 293 to 298 K and the thermo-chemical treatment process using water resulted in a significant reduction in the contact angle measured for distilled water. The studies have also shown that the contact angle is inversely related to surface free energy.

Author Contributions: M.B. performed the analysis of the results; M.N. carried out the tests and wrote the manuscript; W.S. contributed to the concept and modified the manuscript. All authors have read and agreed to the published version of the manuscript.

Funding: This research received no external funding.

Conflicts of Interest: The authors declare no conflict of interest.

References

1. Hatch, J.E. *Aluminum: Properties and Physical Metallurgy*; ASM International: Cleveland, OH, USA, 1984.
2. Khoei, A.R.; Maters, I.; Gethin, D.T. Design optimisation of aluminium recycling processes using Taguchi technique. *J. Mater. Process. Technol.* **2002**, *127*, 96–106. [CrossRef]
3. Vargel, C. *Corrosion of Aluminium*; Elsevier Science: Amsterdam, The Netherlands, 2004.
4. Davis, J.R. *Corrosion of Aluminium and Aluminium Alloys*; ASM International: Novelty, OH, USA, 1999.
5. Hirsch, J.; Skrotzki, B.; Gottstein, G. *Aluminum Alloys: Their Physical and Mechanical Properties*; Wiley-VCH Cerlag Gmbh & Co. KGaA: Weinheim, Germany, 2008.
6. Mondolfo, L.F. *Aluminum Alloys: Structure and Properties*; Elsevier Science: London, UK, 2013.
7. Starke, E.A.; Staley, J.T. Application of modern aluminium alloys to aircraft. *Prog. Aerosp. Sci.* **1996**, *32*, 131–172. [CrossRef]
8. Miller, W.S.; Zhuang, L.; Bottema, J.; Witterbrood, A.J.; De Smet, P.; Haszler, A.; Vieregge, A. Recent development in aluminium alloys for the automotive industry. *Mater. Sci. Eng. A-Struct.* **2000**, *280*, 37–49. [CrossRef]
9. Calcraft, R.C.; Wahab, R.A.; Bottema, J.; Viano, D.M.; Schumann, G.O.; Phillips, R.H.; Ahmed, N.U. The development of the welding procedures and fatigue of butt-welded structures of aluminium-AA5383. *J. Mater. Process. Technol.* **1999**, *92–93*, 60–65. [CrossRef]
10. Poznak, A.; Freiberg, D.; Sanders, P. Chapter 10—Automotive Wrought Aluminium Alloys. In *Fundamentals of Aluminium Metallurgy*; Lumley, R.N., Ed.; Woodhead Publishing: Sawston, UK, 2018; pp. 333–386.
11. Kök, M.; Özdin, K. Wear resistance of aluminium alloy and its composites reinforced by Al_2O_3 particles. *J. Mater. Process. Technol.* **2007**, *183*, 301–309. [CrossRef]
12. Stepniowski, W.J.; Moneta, M.; Karczewski, K.; Michalska-Domanska, M.; Czujko, T.; Mol, J.M.; Buijnsters, J.G. Fabrication of copper nanowires via electrodeposition in anodic aluminum oxide templates formed by combined hard anodizing and electrochemical barrier layer thinning. *J. Electroanal. Chem.* **2018**, *809*, 59–66. [CrossRef]
13. Niedźwiedź, M.; Skoneczny, W.; Bara, M. The influence of anodic alumina coating nanostructure produced on EN AW-5251 alloy on type of tribological wear process. *Coatings* **2020**, *10*, 105. [CrossRef]
14. Bara, M.; Kmita, T.; Korzekwa, J. Microstructure and properties of composite coatings obtained on aluminium alloys. *Arch. Metall. Mater.* **2016**, *61*, 1107–1112. [CrossRef]
15. Kok, M. Production and mechanical properties of Al_2O_3 particle-reinforced 2024 aluminium alloy composites. *J. Mater. Process. Technol.* **2005**, *161*, 381–387. [CrossRef]
16. Kwolek, P.; Drapała, D.; Krupa, K.; Obłój, A.; Tokarski, T.; Sieniawski, J. Mechanical properties of a pulsed anodised 5005 aluminium alloy. *Surf. Coat. Technol.* **2020**, *383*, 1–8. [CrossRef]
17. Zhao, N.-Q.; Jiang, X.-X.; Shi, C.-S.; Li, J.-J.; Zhao, Z.-G.; Du, X.-W. Effects of anodizingconditions on anodic alumina structure. *J. Mater. Sci.* **2007**, *42*, 3878–3882. [CrossRef]
18. Sulka, G.D. *Highly Ordered Anodic Porous Alumina Formation by Self-Organized Anodizing*; Wiley-VCH Verlag GmbH & Co., KGaA: Weinheim, Germany, 2008.
19. Liu, P.; Singh, V.P.; Rajaputra, S. Barrier layer nonuniformity effects in anodized aluminum oxide nanopores on ITO substrates. *Nanotechnology* **2010**, *21*, 115303. [CrossRef] [PubMed]
20. Zhang, L.; Cho, H.S.; Li, F.; Metzger, R.M.; Doyle, W.D. Cellular growth of highly ordered porous anodic films on aluminium. *J. Mater. Sci. Lett.* **1998**, *17*, 291–294. [CrossRef]

21. Aerts, T.; Dimogerontakis, T.; De Graeve, I.; Fransaer, J.; Terryn, H. Influence of the anodizing temperature on the porosity and the mechanical properties of the porous anodic oxide film. *Surf. Coat. Technol.* **2007**, *201*, 7310–7317. [CrossRef]
22. Hao, L.; Cheng, B.R. Sealing processes of anodic coatings—Past, present, and future. *Met. Finish.* **2000**, *98*, 8–18. [CrossRef]
23. Kyungtae, K.; Moonjung, K.; Sung, M.C. Pulsed electrodeposition of palladium nanowire arrays using AAO template. *Mater. Chem. Phys.* **2006**, *98*, 278–282.
24. Bartolome, M.J.; Lopez, V.; Escudero, E.; Caruana, G.; Gonzales, J.A. Changes in the specific surface area of porous aluminium oxide films during sealing. *Surf. Coat. Technol.* **2006**, *200*, 4530–4537. [CrossRef]
25. Hoar, T.P.; Wood, G.C. The sealing of porous anodic oxide films on aluminium. *Electrochim. Acta* **1962**, *7*, 333–353. [CrossRef]
26. Whelan, M.; Cassidy, J.; Duffy, B. Sol–gel sealing characteristics for corrosion resistance of anodised aluminium. *Surf. Coat. Technol.* **2013**, *235*, 86–96. [CrossRef]
27. Bara, M.; Niedźwiedź, M.; Skoneczny, W. Influence of anodizing parameters on surface morphology and surface-free energy of Al_2O_3 layers produced on EN AW-5251 alloy. *Materials* **2019**, *12*, 695. [CrossRef]
28. Zhang, X.; Shi, F.; Niu, J.; Jiang, Y.G.; Wang, Z.Q. Superhydrophobic surfaces: From structural control to functional application. *J. Mater. Chem.* **2008**, *18*, 621–633. [CrossRef]
29. Wang, Q.; Zhang, B.W.; Qu, M.N.; Zhang, J.Y.; He, D.Y. Fabrication of superhydrophobic surfaces on engineering material surfaces with stearic acid. *Appl. Surf. Sci.* **2008**, *254*, 2009–2012. [CrossRef]
30. Xu, X.; Zhu, Y.; Zhang, L.; Sun, J.; Huang, J.; Huang, J.; Chen, J.; Cao, Y. Hydrophilic poly(triphenylamines) with phosphonate groups on the side chains: Synthesis and photovoltaic applications. *J. Mater. Chem.* **2012**, *22*, 4329–4336. [CrossRef]
31. Zhang, Z.; Wu, Q.; Song, K.; Ren, S.; Lei, T.; Zhang, Q. Using cellulose nanocrystals as a sustainable additive to enhance hydrophilicity, mechanical and thermal properties of poly(vinylidene fluoride)/poly(methyl methacrylate) blend. *ACS Sustain. Chem. Eng.* **2015**, *3*, 574–582. [CrossRef]
32. Li, X.; Liu, K.L.; Wang, M.; Wong, S.Y.; Tiju, W.C.; He, C.B.; Goh, S.H.; Li, J. Improving hydrophilicity, mechanical properties and biocompatibility of poly[(R)-3-hydroxybutyrate-co-(R)-3-hydroxyvalerate] through blending with poly[(R)-3-hydroxybutyrate]-alt-poly(ethylene oxide). *Acta Biomater.* **2009**, *5*, 2002–2012. [CrossRef]
33. Ohtsu, N.; Hirano, Y. Growth of oxide layers on NiTi alloy surfaces through anodization innitric acid electrolyte. *Surf. Coat. Technol.* **2017**, *325*, 75–80. [CrossRef]
34. Mokhtari, S.; Karimzadeh, F.; Abbasi, M.H.; Raeissi, K. Development of super-hydrophobic surface on Al 6061 by anodizing and the evaluation of its corrosion behavior. *Surf. Coat. Technol.* **2017**, *324*, 99–105. [CrossRef]
35. Buijnters, J.G.; Zhong, R.; Tsyntsaru, N.; Celis, J.-P. Surface wettability of macroporous anodized aluminum oxide. *ACS Appl. Mater. Interfaces* **2013**, *5*, 3224–3233. [CrossRef]
36. Kim, D.; Hwang, W.; Park, H.C.; Lee, K.-H. Superhydrophobic nanostructures based on porous alumina. *Curr. Appl. Phys.* **2007**, *8*, 770–773. [CrossRef]
37. Tasaltin, N.; Sanli, D.; Jonáš, A.; Kiraz, A.; Erkey, C. Preparation and characterization of superhydrophobic surfaces based on hexamethyldisilazane-modified nanoporous alumina. *Nanoscale Res. Lett.* **2011**, *6*, 487. [CrossRef]
38. Wang, H.; Dai, D.; Wu, C. Fabrication of superhydrophobic surfaces on aluminum. *Appl. Surf. Sci.* **2008**, *254*, 5599–5601. [CrossRef]